

Evolution of a disc-planet system with a binary companion on an inclined orbit

M. Xiang-Gruess¹ * and J.C.B. Papaloizou¹

¹ DAMTP, University of Cambridge, Wilberforce Road, Cambridge CB3 0WA, UK

Accepted . Received ;

ABSTRACT

We study orbital inclination changes associated with the precession of a disc-planet system that occurs through gravitational interaction with a binary companion on an inclined orbit. We investigate whether this scenario can account for giant planets on close orbits highly inclined to the stellar equatorial plane. We obtain conditions for maintaining approximate coplanarity and test them with SPH-simulations. For parameters of interest, the system undergoes approximate rigid body precession with modest warping while the planets migrate inwards. Because of pressure forces, disc self-gravity is not needed to maintain the configuration. We consider a disc and single planet for different initial inclinations of the binary orbit to the midplane of the combined system and a system of three planets for which migration leads to dynamical instability that reorders the planets. As the interaction is dominated by the time averaged quadrupole component of the binary’s perturbing potential, results for a circular orbit can be scaled to apply to eccentric orbits. The system responded adiabatically when changes to binary orbital parameters occurred on time scales exceeding the orbital period. Accordingly inclination changes are maintained under its slow removal. Thus the scenario for generating high inclination planetary orbits studied here, is promising.

Key words: planetary systems: formation – planetary systems: protoplanetary discs – planetary systems: planet-disc interactions

1 INTRODUCTION

In the past few decades, the number of detected extrasolar planets around other main sequence stars has increased dramatically, so that at the time of writing, more than 1000 planets have been discovered. Well studied planet formation scenarios such as core accretion (Mizuno 1980; Pollack et al. 1996) or disc fragmentation (Mayer et al. 2002) involve the planet forming in a disc with the natural expectation that the orbit should be coplanar. However, Rossiter McLaughlin measurements of close orbiting hot Jupiters indicate that around 40% have angular momentum vectors significantly misaligned with the angular velocity vector of the central star (e.g. Triaud et al. 2010; Albrecht et al. 2012). As the stellar and disc angular velocities are naturally expected to be aligned, this would imply an inclination of the planet orbit relative to the nascent protoplanetary disc.

This has been underlined by several recent studies of the interactions of planets with a range of initial orbital inclinations with respect to a disc (e.g. Cresswell et al. 2007;

Marzari & Nelson 2009; Bitsch & Kley 2011). In these works the evolution of planets with masses up to a maximum of $1M_J$ with different initial eccentricities and relatively small initial inclinations up to a maximum of 15° interacting with three-dimensional isothermal and radiative discs are considered. They showed damping for both eccentricity and inclination with the planets circularising in the disc after a few hundred orbits. Planets with higher inclinations have also been studied by e.g. Rein (2012) and Teyssandier et al. (2013). A detailed survey of a range of planet masses and the full range of orbital inclinations interacting with a disc has been presented by Xiang-Gruess & Papaloizou (2013) (hereafter Paper 1). The timescale of realignment with the gas disc was found to be comparable with the disc lifetime for very high inclinations $> 60^\circ$ and planet masses of one Jupiter mass. For smaller initial relative inclinations and/or larger planet masses, the timescale for realignment is shorter than the disc lifetime. These results taken together imply that there is a need for an explanation for the origin of misaligned giant planets, if it is assumed that the discs angular momentum vector is always aligned with the spin axis of the central star.

* E-mail: mx216@cam.ac.uk

Several scenarios have been proposed to explain the origin of misalignments between the planetary orbital angular momentum vector and the stellar rotation axis as well as produce close in giant planets. The first involves excitation of very high eccentricities, either through the Lidov-Kozai effect induced by the interaction with a distant companion (e.g. Fabrycky & Tremaine 2007; Wu et al. 2007), or through planet-planet scattering or chaotic interactions (e.g. Weidenschilling & Marzari 1996; Rasio & Ford 1996; Papaloizou & Terquem 2001; Nagasawa et al. 2008). When the planet attains a small enough pericentre distance, this is then followed by orbital circularization due to tidal interaction with the central star, leaving the planet on a close inclined circular orbit.

A method for producing high disc inclinations with respect to the stellar equator has also been indicated by Thommes & Lissauer (2003), who have studied the evolution of two giant planets in resonance, adopting an approximate analytical expression for the influence of a gas disc in producing orbital migration. Their calculations suggest that resonant inclination excitation can occur when the eccentricity of the inner planet reaches a threshold value ~ 0.6 . Inclinations gained by the resonant pair of planets can reach values up to $\sim 60^\circ$.

However in a recent study, Dawson et al. (2012) find that large eccentricities, that are expected to be associated with such interactions for orbits too wide to be affected by stellar tides, are seen mostly in metal rich systems. Accordingly they conclude that gentle disc migration and planet-planet scattering must both operate during the early evolution of giant planets. Only systems packed with giant planets, which most easily form around metal rich stars, can produce large eccentricities through scattering. They also note a lack of a correlation between spin-orbit misalignment and metallicity that may indicate the operation of a mechanism that can cause misalignment of the disc while simultaneously allowing disc migration of giant planets into close orbits.

An explanation for the origin of misaligned planets, that is consistent with formation in and inward migration driven by a disc may be connected with the possibility that the orientation of the disc changes, possibly due either to a lack of orbital alignment of the source material or to gravitational encounters with passing stars. This may occur either before or after planet formation (e.g. Bate et al. 2010; Thies et al. 2011).

Thies et al. (2011) showed that the capture of gas from accretion envelopes by a protoplanetary disc could cause it to become significantly misaligned with respect to its original plane. Although no planets are involved in their simulations, it is of interest to remark that misaligned gas discs can easily be produced when interactions with the environment out of which they form are considered. In this regard we note that protostars are not generally isolated but are bound in stellar clusters where gravitational interactions are common.

Recently, the system Kepler-56 has been studied by Huber et al. (2013) who used asteroseismological methods to determine the obliquity in that system. Kepler-56 has two known transiting planets. Huber et al. (2013) found that the planets have angular momentum vectors strongly inclined with respect to the central stellar spin axis. Taking into account the large observed obliquities, dynamical simulations with the two known planets failed to produce a stable non

coplanar planetary system. The authors then studied an alternative scenario involving a distant companion and were able to show in dynamical simulations that they succeeded in producing the architecture of the Kepler-56 system including coplanarity of the planetary orbits and the high obliquity. Further observations are required to specify the mass of the companion which is crucial to determine the origin of the misalignment in Kepler-56. In the case of a planetary companion, the misalignment is inferred to occur after the planets have formed while in the case of a stellar companion, the misalignment is inferred to occur while the host gaseous disc is present.

In this context, Batygin (2012) suggested that a binary companion could be responsible for producing misalignments between stellar spin axes and planetary orbital planes as a result of making the protoplanetary disc precess. The process envisaged the formation and disruption of wide binaries in birth clusters. that dissolve on timescales up to a few tens of millions of years. The excitation of significant misalignment should then occur within the same time scale.

We remark that the interaction between a binary companion and a disc could cause the disc to become warped. Notably, Terquem (2013) studied the effect of a warped disc on the orbit of a Jupiter mass planet. For a sufficiently warped disc, it was shown that a high orbital inclination for the planet might be excited through direct gravitational interaction.

In view of the above discussion, it is important to investigate the response of a system composed of both a protoplanetary disc and one or more planets that can induce a gap and migrate within it, under the gravitational perturbation of a binary companion in a misaligned orbit. If misalignment with the stellar equatorial plane is induced during the late stages, planets may reside in a cavity in the inner regions of the disc, relatively little further accretion of disc material onto the central star may take place optimising the final misalignment, thus making this an interesting case to study.

In this paper we consider the response of the disc-planet system as a whole obtaining conditions, based on estimates of precessional torques, for it to maintain approximate coplanarity and test these against the results of numerical simulations. From these we are able to show that for appropriate parameters of interest, the whole system precesses approximately as a rigid body with the disc exhibiting only a modest amount of warping. This does not necessitate a self-gravitating disc as assumed by Batygin (2012) because the disc can communicate more effectively through the action of pressure forces (eg. Larwood et al. 1996) than through density waves as long as the Toomre stability parameter exceeds unity, a situation expected for the most part during the later stages of protoplanetary discs (see Papaloizou & Lin 1999, for a detailed discussion). Even if the outer parts of the disc are maintained close to marginal stability, effects due to self-gravity and pressure are expected to be comparable for global warps. Accordingly we make the simplification of neglecting the disc self-gravity which results in a very significant reduction in computational resource requirements. We also test how the response adjusts to changes in the orbital parameters of the binary finding that this is essentially adiabatic even when the changes occur on a timescale comparable to the binary orbital period.

It has been shown that Smoothed particle hydrody-

namics (SPH) simulations are capable of being applied to the problem of planet-disc interaction (e.g. Schäfer et al. 2004; de Val-Borro et al. 2006) though in comparison to grid-based simulation methods, they are generally more diffusive and incur greater computational expense. But in contrast to grid-based methods, as they adopt a Lagrangian approach, SPH simulations can be readily used to simulate a gas disc with a free boundary that undergoes a large amount of movement in three dimensions with the disc having the freedom to change its shape at will. As it is suitable for a system precessing with high mutual inclinations, we adopt this approach here.

In Section 2, we describe our simulation technique, giving details of the modified locally isothermal equation of state we adopted in Section 2.1 and details of the smoothing length and artificial viscosity prescriptions in Section 2.2. In Section 3, we describe the general setup for the disc, the planets, the central star and the binary companion. In Section 4, we give a brief theoretical overview of the global interaction between the planet-disc system and a binary star with orbital plane misaligned with the disc midplane. Estimates of the precessional torques that can act between different components in the system are given in appendix A. If the putative precession frequencies they could produce, significantly exceed the putative precession frequency of the entire system calculated assuming that it rotates as a rigid body, these torques can be utilised to maintain alignment. Precessional Torques acting between a disc and a planet in a gap/inner cavity as well as between two planets without a disc are considered.

We go on to present the results of our simulations in Section 5. Simulations with a disc together with a single migrating giant planet and a binary companion in an inclined orbit are discussed in Section 5.1. These systems are found to maintain approximate alignment consistently with estimated magnitudes of internal precessional torques. The adiabatic response to changes in the binary orbit is discussed in Section 5.4. A simulation with a disc, misaligned binary orbit and a three planet system is described in Section 6. The disc-planet system is seen to maintain approximate coplanarity, as a result of disc-planet torques, as in the single planet case, even though there is a phase of dynamical instability. Finally, we summarize and discuss our results in Section 7.

2 SIMULATION DETAILS

We have performed simulations using a modified version of the publicly available code GADGET-2 Springel (2005). GADGET-2 is a hybrid N-body/SPH code capable of modelling both fluid and distinct fixed or orbiting massive bodies. In our case the central star, of mass M_* , is fixed while the planets, of masses $M_{p,i}$, $i = 1, 2..$ and the binary companion, of mass M_B orbit as distinct massive bodies. We adopt spherical polar coordinates (r, θ, ϕ) with origin at the centre of mass of the central star. The associated Cartesian coordinates (x, y, z) are such that the (x, y) plane coincides with the initial midplane of the disc.

The gaseous disc is represented by SPH particles. An important issue for N-body/SPH simulations is the choice of the gravitational softening lengths. In our simulations, the massive bodies (i.e. central star, companion and the planets) are

unsoftened when interacting with each other, allowing them to undergo realistic close encounters.

The total unsoftened gravitational potential Ψ at a position \mathbf{r} is given by (see also Papaloizou & Terquem 1995; Larwood et al. 1996).

$$\Psi(\mathbf{r}) = -\frac{GM_*}{|\mathbf{r}|} - \frac{GM_B}{|\mathbf{r} - \mathbf{D}|} + \frac{GM_B \mathbf{r} \cdot \mathbf{D}}{|\mathbf{D}|^3} - \sum_i \left(\frac{GM_{p,i}}{|\mathbf{r} - \mathbf{r}_{p,i}|} - \frac{GM_{p,i} \mathbf{r} \cdot \mathbf{r}_{p,i}}{|\mathbf{r}_{p,i}|^3} \right). \quad (1)$$

Contributions from the central star, the binary companion of mass, M_B , with position \mathbf{D} , together with an arbitrary number of planets with masses, $M_{p,i}$, and position vectors $\mathbf{r}_{p,i}$, that are summed over, are included. Because the origin of the coordinate system moves with the central star, the well known indirect terms accounting for the acceleration of the coordinate system are present in equation (1).

For the computation of the gravitational interaction between the massive bodies and the SPH particles, the potential was softened following the method of Springel (2005). This was implemented with fixed softening lengths $\varepsilon_* = \varepsilon_B = 0.4$ AU and $\varepsilon_p = 0.1$ AU for the central star, and the binary companion and planets, respectively.

The disc acts gravitationally on the other bodies, but its self-gravity was neglected as this is not expected to play a significant role for protoplanetary discs of the mass we consider. For the computation of the gravitational force between the disc and the planets, we included all SPH particles in order to enable an accurate calculation when applying the tree algorithm.

The stars and the planets are allowed to accrete gas particles that approach them very closely. We followed the procedure of Bate et al. (1995) (see also Paper 1). This was applied such that for the stars and planets, the outer accretion radii were fixed during the simulation to be $R_{accr,*} = R_{accr,B} = 7 \times 10^{11}$ cm, and $R_{accr,p} = 7 \times 10^{10}$ cm, respectively. The inner accretion radii were taken to be 0.5 of the outer accretion radii. In practice, for the equations of state we used, the accretion of gas particles was found to play only a minor role in our simulations, producing negligible change to the masses of the planet and both stars.

2.1 Equation of state

As described in Paper 1, we adopt a locally isothermal equation of state (EOS) incorporating the modification of Peplinski et al. (2008). The sound speed c_s is obtained from

$$c_s = \frac{h_s r_s h_p r_p}{[(h_s r_s)^n + (h_p r_p)^n]^{1/n}} \sqrt{\Omega_s^2 + \Omega_p^2}, \quad (2)$$

with $n = 3.5$. Here $r_s = |\mathbf{r}|$ and $r_p = |\mathbf{r} - \mathbf{r}_{p,i}|$ are the distances to the central star and the nearest planet respectively. Here $h_s = H/r_s$ is the disc aspect ratio with H being the circumstellar disc scale height. The angular velocities in the circumstellar and circumplanetary discs are Ω_s and Ω_p respectively. We evaluate these assuming Keplerian circular orbits, thus they are given by

$$\Omega_s = \sqrt{\frac{GM_*}{r_s^3}} \quad \text{and} \quad \Omega_p = \sqrt{\frac{GM_{p,i}}{r_p^3}} \quad \text{respectively.} \quad (3)$$

For $r_s \leq 10$ AU, we adopt $h_s = 0.05$. For simulations with a binary companion in an orbit inclined to the disc, it was found that for high initial inclinations $i_B \geq 60^\circ$, expansion of the outer regions of the disc could result in a small number of particles being induced to interact strongly with the companion. In order to avoid numerical problems arising from this, we adopted the following procedure. For the outer parts with $20 \text{ AU} > r_s > 10 \text{ AU}$, we applied a linear decrease of h_s to 0.03. For $r \geq 20$ AU, we adopted a constant ratio $h_s = 0.03$. We found that the application of this procedure did not affect results for smaller values of $i_B < 60^\circ$. Accordingly it was not adopted for the simulations of the multi-planet system presented below. Here we only study planet masses $M_{p,i} \geq 1 M_J$ for which the aspect ratio of the circumplanetary disc is taken to be $h_p = 0.6$ (see paper 1 for more discussion).

2.2 Smoothing length and artificial viscosity

For our SPH calculations, the smoothing length was adjusted so that the number of nearest neighbours to any particle contained within a sphere of radius equal to the local smoothing length was 40 ± 5 . The pressure is given by $p = \rho c_s^2$. Thus apart from the vicinity of a planet, the temperature in the disc is $\propto r^{-1}$. The artificial viscosity parameter α of GADGET-2 (see equations (9) and (14) of Springel 2005) was taken to be $\alpha = 0.5$.

We remark that the artificial viscosity is modified by the application of a viscosity-limiter to reduce artificially induced angular momentum transport in the presence of shear flows. This is especially important for the study of Keplerian discs. Details are given in Paper 1. Also in Paper 1, we showed that runs with $\alpha = 0.5$ provided the best match to the analytic ring spreading solution with the Shakura & Sunyaev (1973) viscosity parameter $\alpha_{SS} = 0.02$. SPH simulations accordingly model a viscous disc, with a viscosity that behaves like a conventional Navier Stokes viscosity in that context. However, it is important to note the effective viscosity is likely to be flow dependent and so there may not be a particular form that applies to general situations.

3 INITIAL CONDITIONS

We study a system composed of a central star of one solar mass M_\odot , a binary companion of mass $M_B = 1 M_\odot$, a gaseous disc and one or three planets initially embedded in the disc. The disc is set up such that the angular momentum vector for all particles was in the same direction enabling a midplane for the disc to be defined. For simulations with a single planet, the planet mass was taken to be $M_{p,1} = 2 M_J$ unless otherwise stated. For the simulation with three planets, we chose planet masses in the range $[0.4, 2] M_J$. The planets were initiated in circular coplanar orbits with zero inclination with respect to the initial disc midplane in all cases.

The primary central star is fixed at the origin of our coordinate system while the binary star with separation D orbits in a circle about the primary central star with orbital

angular velocity

$$\omega_B = \sqrt{\frac{2GM_\odot}{D^3}} \quad (4)$$

with $D = |\mathbf{D}|$. The gravitational effect of the disc and planets on the binary orbit is neglected. In order to avoid transients arising from an abrupt introduction of the binary star, we allow its mass to increase linearly to $1 M_\odot$ during the first 10 internal time units, with the internal time unit being the orbital period at $a = 5$ AU. Corresponding to this, the internal unit of length is taken to be 5 AU. These units of length and time are adopted for all plots shown in this paper.

The particle distribution was chosen to model a disc with surface density profile given by

$$\Sigma = \Sigma_0 R^{-1/2}. \quad (5)$$

Here Σ_0 is a constant and R is the radial coordinate of a point in the midplane. This applied to the radial domain $[0, R_{out} - \delta]$, with $R_{out} = 4a$ and $\delta = 0.4a$. A taper was applied such that the surface density was set to decrease linearly to zero for R in the interval $[R_{out} - \delta, R_{out} + \delta]$. Disc material thus occupies the radial domain $[0, R_{out} + \delta]$.

The disc mass is given by

$$M_D = 2\pi \int_{R_{in}}^{R_{out}} \Sigma(r) r dr = \frac{4}{3} \pi \Sigma_0 R_{out}^{3/2}, \quad (6)$$

which is used to determine Σ_0 . For the simulations presented here, we adopted $M_D = 10^{-2} M_\odot$. The disc particles were set up in a state of pure Keplerian rotation according to

$$v_\varphi = \sqrt{r_s \frac{d\Phi_*}{dr_s}}, \quad (7)$$

where Φ_* is the gravitational potential due to the central star. In the innermost region around the central star, the disc properties (e.g. Ω_s and accordingly c_s) are modified by the softening of the potential due to the central star. For this reason simulations are terminated if migrating planets move inwards to the extent that the dynamics starts to become affected by this region.

The number of SPH particles for most of our simulations was taken to be 2×10^5 . This enabled a suite of simulations to be carried out for up to 600 orbits in our dimensionless units. This length of time was required to study the precession of the disc. Some of our simulations were also run with 10^5 and 4×10^5 particles in order to test the effect of changing particle number. No significant changes occurred. This situation is the same as was indicated for the simulations presented in Paper 1.

For orbital separation of the binary star, we adopted $D = 100$ AU. This is distant enough to result in a regular almost rigid body precession of the disc, while being close enough to yield a short enough precession period that the disc precession could be studied. We consider values of the inclination i_B of the binary star with respect to the $z = 0$ plane in the reference frame of the host star in the range $[0, \pi/2]$. In this context we remark that as the induced precession of the disc-planet system is consistent with a secular interaction it should have little dependence on the sense of rotation of the binary in its orbit, so that additional values of i_B in the interval $[\pi/2, \pi]$ do not need to be considered.

We remark that for i_B approaching $\pi/2$, the disc angular momentum vector may almost completely reverse relative to its initial direction given a sufficiently long time.

4 INFLUENCE OF A BINARY COMPANION ON THE DISC AND PLANETS

In this section we consider the precession of the disc induced by the binary companion and how torques between the disc and an inner planet and subsequently between two planets can enable the system as a whole to precess approximately as a rigid body.

4.1 Torque acting on the disc due to a binary companion

The response of the disc, with no planets present, to a binary perturber in an inclined circular orbit has been studied by eg. Papaloizou & Terquem (1995) and Larwood et al. (1996). Adopting their formalism, we obtain the precession frequency of a disc with our surface density profile. This is appropriate when the disc is able to communicate with itself, either through wave propagation or viscous diffusion, on a time-scale less than the inverse precession frequency. In that case the disc precesses approximately like a rigid body. This is found to be the case for our simulations (see below). The precession is retrograde with period $2\pi/\omega_0$, where ω_0 is given by (see Eq. 21 in Larwood et al. 1996)

$$\omega_0 = \left(\frac{3GM_B}{4D^3} \right) \cos i_B \frac{\int_{R_{in}}^{R_{out}} \Sigma r^3 dr}{\int_{R_{in}}^{R_{out}} \Sigma r^3 \Omega dr} \quad (8)$$

We remark that this takes account of only the quadrupole term in the expansion of its time averaged perturbing potential due to the companion. Neglecting any evolution of the disc surface density profile making the approximation of extending the disc radial domain to $[0, R_{out}]$, and adopting Kepler's law such that $\Omega^2(R) = GM_*/R^3$, we obtain

$$\omega_0 = \left(\frac{3GM_B}{7D^3} \right) \cos(i_B) \frac{1}{\Omega(R_{out})} \quad (9)$$

or equivalently

$$\frac{\omega_0}{\Omega(R_{out})} = \left(\frac{3M_B R_{out}^3}{7M_* D^3} \right) \cos(i_B) \quad (10)$$

For $M_B/M_* = 1$, $D/R_{out} = 5$ and $i_B = \pi/4$, Eq. (10) gives $\omega_0/\Omega(R_{out}) = 0.0024$. Therefore, the condition for sound to propagate throughout the disc during a precession time, namely $H/R > \omega_0/\Omega(R_{out})$, is well satisfied for our simulations. This is the condition for approximate rigid body precession when the disc is in the bending wave regime. This occurs for the viscosity parameter $\alpha_{SS} < H/R$, which should be applicable here (see Larwood et al. 1996, and Paper 1). Numerically, we find that $\Omega(R_{out}) = 2.22 \times 10^{-9} \text{s}^{-1}$. and $\omega_0 = 0.0024 \times 2.22 \times 10^{-9} \text{s}^{-1} = 5.3 \times 10^{-12} \text{s}^{-1}$. The precession period is accordingly, $T_p = 2\pi/\omega_0 \sim 1.19 \times 10^{12} \text{s} \sim 37709 \text{yr}$ or in 3373 time units. We remark that as $\omega_0 \propto D^{-3}$, this implies that binaries with separations up to 400 AU could have significant effects over typical protoplanetary disc lifetimes.

4.2 Torques between the different components of the system and the maintenance of approximate coplanarity

When planets are present together with the disc, torques act between them, as well as between the planets and the disc. The torque due to the binary companion acts mainly on the outer parts of the disc. Its effect may be communicated to planets in the inner disc regions through the action of these additional torques. In appendix A, we derive expressions for them together with the precession frequencies they induce, assuming that the angular momentum vectors of the different components are approximately aligned. Here, we use these expressions to estimate whether the precessional torques are large enough in magnitude to allow approximate coplanarity to be maintained. As indicated in appendix A, this requires that the magnitudes of the characteristic precession frequencies that could be induced by the additional torques be significantly larger than the magnitude of the precession frequency induced by the binary companion.

The retrograde precession rate induced in the orbit $M_{p,2}$, with radius $r_{p,2}$, by the disc can be estimated from (A10) of appendix A to be

$$\frac{\omega_{p2}}{\Omega_0} \sim \frac{3M_D}{4M_\odot} \frac{r_{p,2}^{3/2} R_0^{3/2}}{(R_{out} R_{in,d})^{3/2}}, \quad (11)$$

where we have expressed the precession frequency in units of the orbital frequency, Ω_0 , at the reference radius R_0 used to define our dimensionless units.

For our simulations we adopt $R_0 = R_{in,d} = 5 \text{ AU}$, $R_{out} = 20 \text{ AU}$, $M_D = 10^{-2} M_\odot$ and a simple model with the presence of a gap and the planet residing in an inner cavity with $r_{p,2} = 0.8R_{in,d}$. We then find $\omega_{p2}/\Omega_0 \sim 6.7 \times 10^{-4}$. In addition, direct numerical evaluation using equations (A5) and (A9) indicates this estimate should be increased by a factor of 2.3. For our simulations we have $\omega_0/\Omega_0 < \sim 4 \times 10^{-4}$, thus the above discussion indicates that ω_{p2} may significantly exceed ω_0 , and so torques acting between the planet and disc are potentially able to maintain uniform precession.

In the case of a planetary system, the innermost planets, being more distant from most of its mass distribution, are less affected by disc. However, uniform precession may be maintained through torques due to other planets. We now suppose $M_{p,2}$ is acted on by an exterior planet $M_{p,1}$. Using equation (A11) we estimate the precession frequency induced by $M_{p,1}$ on $M_{p,2}$ to be

$$\frac{\omega_{p2}}{\Omega_0} = \frac{M_{p,1} r_{p,2}^{1/2} R_0^{3/2}}{4M_\odot r_{p,1}^2} b_{3/2}^1(r_{p,2}/r_{p,1}). \quad (12)$$

Taking $M_{p,1} = 2 \times 10^{-3} M_\odot$, $r_{p,1} = R_0$ and $r_{p,2}/r_{p,1} = 0.6$, corresponding to proximity to the 2:1 resonance, we obtain $\omega_{p2}/\Omega_0 = 1.25 \times 10^{-3}$. Thus we again conclude that torques induced by $M_{p,1}$ on $M_{p,2}$ are potentially able to maintain uniform precession.

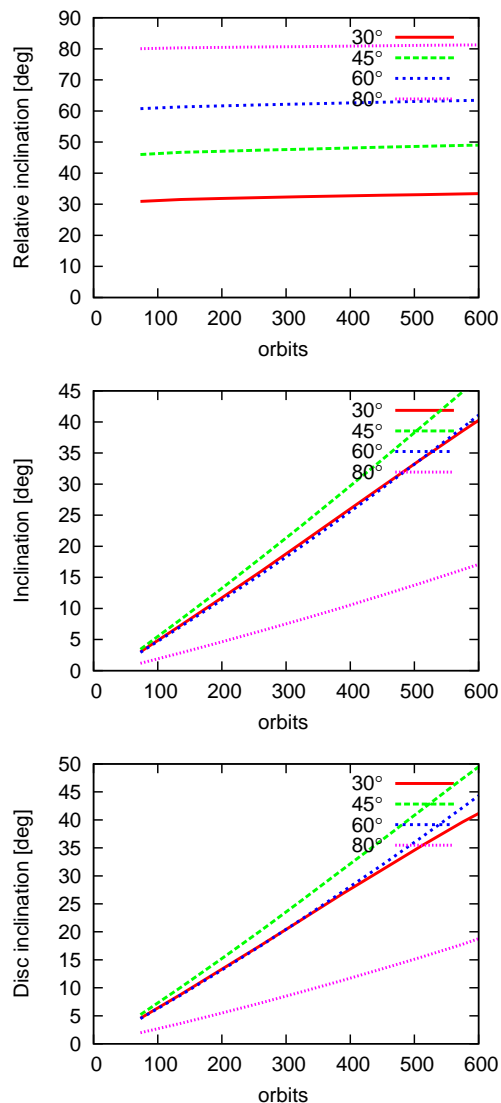


Figure 1. Inclination of the angular momentum vector of the planet with respect to that of the binary companion (top panel), inclination of the planetary orbit and the disc with respect to the (x, y) plane, the original disc midplane, as functions of time (middle and bottom panel respectively) for different inclinations i_B of the binary orbit.

5 SIMULATION RESULTS

5.1 Single planet in the presence of a gas disc

We study the evolution of a single planet of mass $2 M_J$ in the presence of a gas disc for different initial inclinations, i_B , of the binary companion to the initial midplane of the disc. We show the dynamical evolution of the planet-disc system for $i_B = 30^\circ$, $i_B = 45^\circ$, $i_B = 60^\circ$ and $i_B = 80^\circ$. Simulations were run for 600 orbits because beyond this point the inwardly migrating planet started to become affected by particles that accumulated in the innermost boundary region in the vicinity of the central star. We plot a variety of inclination angles as defined below.

The orbital inclination of the planet is measured with

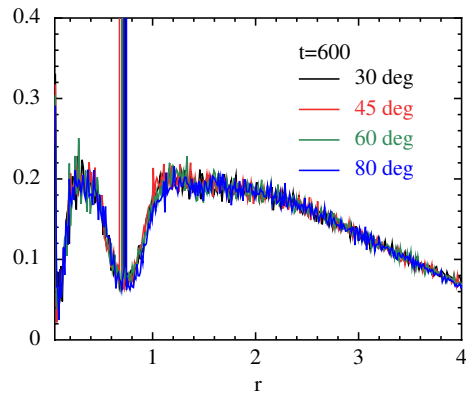


Figure 2. Surface density for a gaseous disc together with a $2 M_J$ planet in the presence of an inclined binary star of mass $1 M_\odot$ for different values of i_B . The different curves almost coincide. The spike at the location of the planet is due to gas bound to it. The indicated coordinate, r , is the distance to the central star.

respect to the (x, y) plane. It is thus given by

$$i_p = \arccos\left(\frac{\mathbf{L}_{p,z}}{|\mathbf{L}_p|}\right), \quad (13)$$

where \mathbf{L}_p is the angular momentum vector of the planet and $\mathbf{L}_{p,z}$ its z -component. The relative inclination, $i_{rel,p}$, of the planetary orbit to the binary orbit is then obtained from

$$i_{rel,p} = \arccos\left(\frac{\mathbf{L}_p \cdot \mathbf{L}_B}{|\mathbf{L}_p| \cdot |\mathbf{L}_B|}\right), \quad \text{where} \quad (14)$$

$$\mathbf{L}_B = M_B(\mathbf{r}_B \times \mathbf{v}_B),$$

is the angular momentum vector of the binary star which does not vary with time on account of the orbit being fixed.

The disc inclination measured with respect to the (x, y) plane is obtained from

$$i_D = \arccos\left(\frac{\mathbf{L}_{D,z}}{|\mathbf{L}_D|}\right), \quad \text{where} \quad (15)$$

$$\mathbf{L}_D = \sum_i m_i(\mathbf{r}_i \times \mathbf{v}_i),$$

is the total angular momentum of the disc obtained by summing the contributions from each active particle and $\mathbf{L}_{D,z}$ is its z component.

Figure 1 shows the inclination of the angular momentum vector of the planet with respect to that of the binary, and the inclination of the planetary orbit and the disc with respect to the (x, y) plane as a function of time for $i_B = 30^\circ$, $i_B = 45^\circ$, $i_B = 60^\circ$ and $i_B = 80^\circ$. It will be seen that the relative inclination of the planet and binary companion orbits is almost constant for the entire simulation period. Furthermore the evolution of the inclination of the planetary orbit with respect to the (x, y) plane is very similar to that of the disc inclination with respect to the same plane for all values of i_B . This indicates that the planetary orbit and disc remain coplanar during the entire simulation for all inclinations of the binary orbit studied. In each case the inclinations with respect to the (x, y) plane are seen to increase approximately linearly with time. This will be seen to be a consequence of the approximately uniform precession of the disc-planet system. It means that the system becomes increasingly misaligned with respect to its original

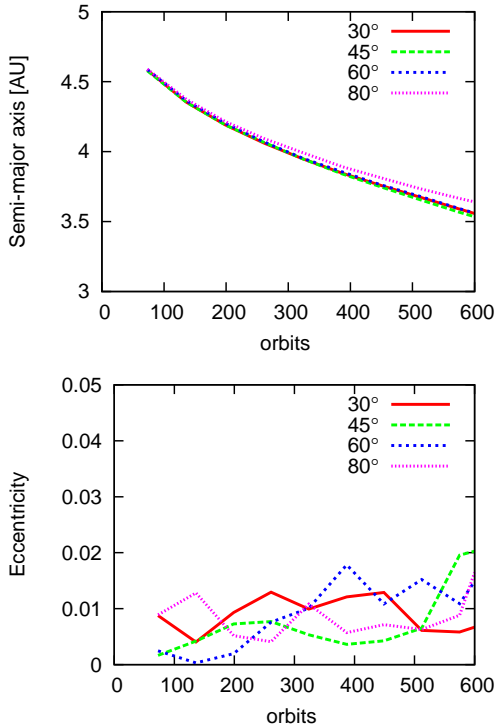


Figure 3. The evolution of the planetary semi-major axis a_p (upper panel) and eccentricity e_p (lower panel) for the simulations shown in Fig. 2. Little variation with i_B is seen.

plane. The latter could coincide with the equatorial plane of the central star.

The amount of inclination increase after a given time is a function of i_B . If this angle is β , we have $\sin \beta/2 = \sin i_B \sin \omega_0 t/2$ assuming rigid body precession. Then from equation (8) we see that the amount of evolution after a given time is initially expected to be proportional to $\omega_0 \sin i_B$, or $\sin 2i_B$. This assumes a linear increase with time, which is expected to be an accurate approximation (to within at most a few % as long as the inclination change is less than $\sim 50^\circ$, as is the case for the results in Fig. 1 at the latest times. It is apparent that the largest inclination change occurs for $i_B = 45^\circ$, attaining $\sim 50^\circ$ by the end of the simulation. We remark that this implies a precession period that is reasonably consistent with equation (10) (see also the discussion below and in Section 4.1) confirming our simple modelling approach.

In confirmation of the above discussion, the inclinations for $i_B = 30^\circ$ and $i_B = 60^\circ$ are seen to increase in almost the same way as expected. Furthermore, the inclination changes approximately three times slower for $i_B = 80^\circ$ as compared to $i_B = 45^\circ$. This is approximately equal to the expected value of $(\sin 160^\circ)^{-1}$.

Since the planet and the disc remain approximately coplanar for all inclinations i_B of the binary orbit, the mass surface density profile of the disc is also very similar in all inclination cases, as is clearly illustrated in Figure 2. Notably, the structure of the gap induced by the planet hardly varies.

Fig. 3 shows the evolution of the semi-major axis a_p and eccentricity e_p of the planet. Since for all studied i_B , the

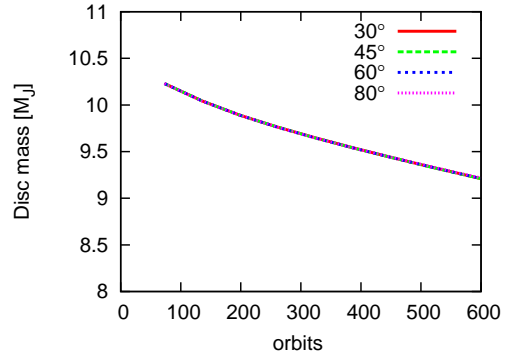


Figure 4. The evolution of the disc mass over 600 orbits. The behaviour for different inclinations is almost identical.

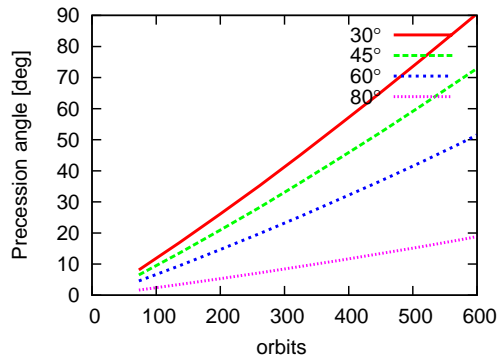


Figure 5. The evolution of the precession angle β_p for the simulations shown in Fig. 2. These are approximately consistent with a uniform precession rate $\propto \cos i_B$.

planetary orbit and disc are approximately coplanar with essentially the same surface density distribution and gap profile, the evolution of the semi-major axis is expected to be the same for all i_B . This is confirmed in Figure 3. The planet is seen to migrate inwards from 5 AU to 3.5 AU during the course of the simulation. In addition no significant eccentricity is generated in the planetary orbit which is a common feature of the simulations presented here.

The disc mass shown in Figure 4 decreases from 10 M_J at the simulation start to roughly 9 M_J after 600 orbits. This evolution is typical for all simulations shown in this paper.

Fig. 5 shows the evolution of the precession angle of the disc angular momentum vector, \mathbf{L}_D , around the angular momentum vector of the binary star, \mathbf{L}_B , for different i_B . The precession angle of the disc, $\beta_p(i_B)$, regarded as a function of i_B , is defined as

$$\cos \beta_p = \frac{\mathbf{L}_D \times \mathbf{L}_B}{|\mathbf{L}_D \times \mathbf{L}_B|} \cdot \mathbf{u} \quad (16)$$

(See also the definition of β_p in Larwood et al. 1996). For \mathbf{u} , any fixed unit reference vector in the (x, y) plane could be used. In our case, we made the following choice:

$$\mathbf{u} = \frac{\mathbf{L}_{D,0} \times \mathbf{L}_B}{|\mathbf{L}_{D,0} \times \mathbf{L}_B|}, \quad (17)$$

where $\mathbf{L}_{D,0}$ is the total disc angular momentum at time $t = 0$. Assuming the presence of the planet can be neglected and that we have rigid body precession induced by the time av-

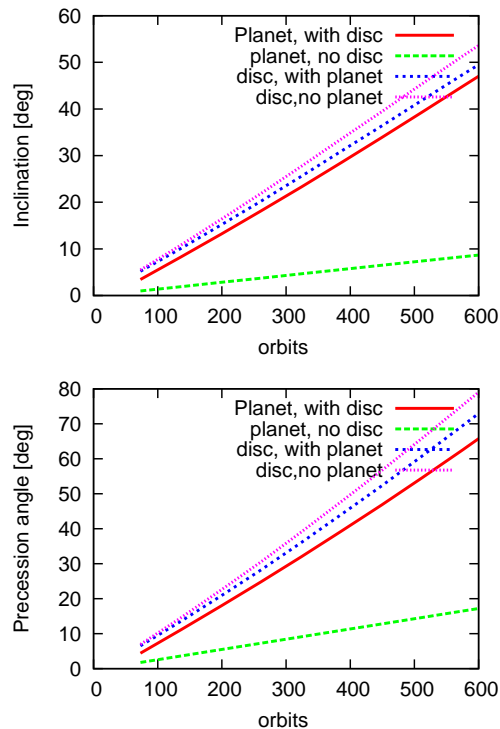


Figure 6. Study of the coupling between disc and planet for $i_B = 45^\circ$. The evolution of the inclinations of the disc and planetary orbit with respect to the (x, y) plane for three simulations are shown in the upper panel. See the text for the allocation of the different curves. The evolution of the corresponding precession angles is indicated in the lower panel.

eraged gravitational potential of the binary companion, the precession rate is expected to be proportional to $(\cos i_B)^{-1}$. After 600 orbits, the precession angles are found to be $\beta_p(30^\circ) = 90^\circ$, $\beta_p(45^\circ) = 72^\circ$, $\beta_p(60^\circ) = 50^\circ$, $\beta_p(80^\circ) = 20^\circ$. Thus $\beta_p(30^\circ)/\beta_p(45^\circ) = 1.25$ which is in good agreement with the theoretical expectation of $\cos 30^\circ/\cos 45^\circ \cong 1.2$. Similarly, $\beta_p(60^\circ)/\beta_p(80^\circ) = 2.5$ as against the expected value $\cos 60^\circ/\cos 80^\circ \cong 2.9$. Also the comparison between the two extreme cases $\beta_p(30^\circ)/\beta_p(80^\circ) = 4.5$ shows a satisfactory agreement with the theoretical expectation of $\cos 30^\circ/\cos 80^\circ \cong 5$.

But note that the results illustrated in Fig. 5 indicate that the precession frequency increases very slowly with time. This evolution is an expected consequence of the accretion, together with the outward expansion, of disc material. Even though the disc mass distribution changes with time, the system continues to undergo approximate rigid body precession.

5.2 Influence of the gas disc and a single planet upon each other

In the simulations described above, the planet and disc are coupled to each other such that the planetary orbit and disc midplane remain approximately coplanar independently of which i_B we chose. We now study the influence of the gas disc and the planet on each other in more detail for $i_B = 45^\circ$. In the upper panel of Fig. 6, we show the evolution of

various inclinations for three different simulations. The first of these was the simulation of the planet, disc and binary companion described above. The second was a simulation with only the disc and binary companion, and the third was a simulation with only the planet and binary companion. Thus the planet was omitted in the second simulation and the disc was omitted in the third simulation. The red line shows the evolution of the planetary orbit inclination with respect to the (x, y) plane in the first simulation, while the blue dotted line shows the corresponding inclination of the disc in the same simulation. Both show a very similar evolution on account of the strong coupling between the planet and disc. The purple dotted line shows the evolution of the disc inclination for the second simulation without the planet and the green line shows the evolution of the planetary orbit inclination for the third simulation for which the disc was omitted. It is seen clearly that the disc inclination evolution without a planet is similar to the disc inclination evolution with a planet. In contrast, the evolution of the planetary orbit inclination in the absence of the gas disc is significantly different to the evolution that occurs when the gas disc is present. In fact the evolution in the latter case is very much slower because the interaction of the planet with the binary companion when the disc is absent is very much weaker than the interaction of the disc with the binary companion independently of whether the planet is present. These results clearly indicate the strong coupling between planet and disc when both are present.

This can be confirmed by considering the evolution of the precession angles shown in the lower panel of Fig. 6. While the evolution for the disc is almost independent of the presence of the planet, the evolution for the planet in the combined system differs significantly from the evolution in the absence of the gas disc. In the presence of the disc, the planet's precession angle after 600 orbits is $\beta_p = 65^\circ$ while in the absence of the disc, it has only reached $\beta_p = 18^\circ$ being almost four times smaller.

In order to indicate the evolution of the geometrical form of the disc in the first simulation, we show the surface density of the disc projected onto the (x, z) and (y, z) planes in Fig. 7. after $t = 0$, $t = 300$, and $t = 600$ orbits. These plots indicate only weak warping of the disc as its orientation changes. This is a recurrent feature of the simulations presented here. The near coplanarity of the planetary orbit is indicated by the fact that the planet is always seen to be close to the disc midplane.

The above results lead to the conclusion that it is the disc which dominates the evolution of the whole disc-planet system. The orientation of the planetary orbit just follows the disc, maintaining a near coplanar orientation while a gap is maintained inside the disc.

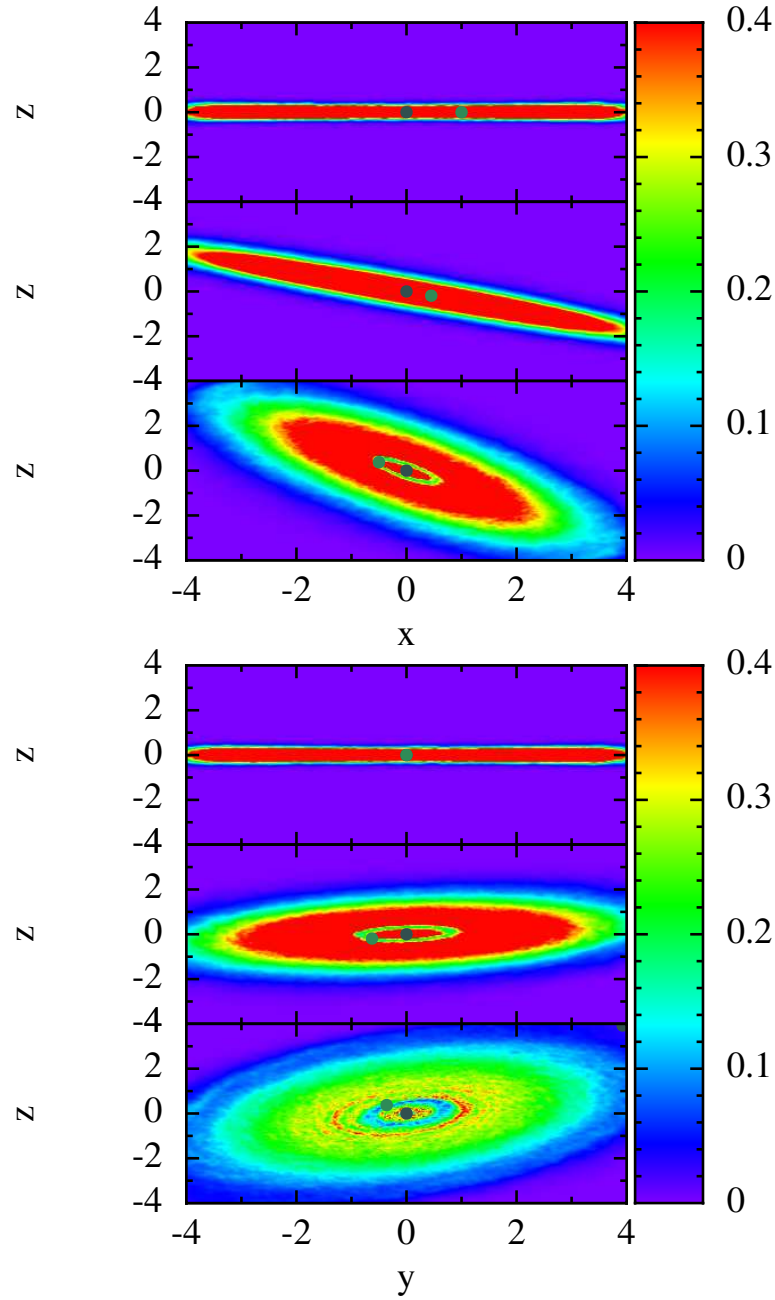


Figure 7. The surface density of the disc on the (x, z) plane (upper set of three plots) and the (y, z) plane (lower set of three plots) for the simulation with disc and planet illustrated in Fig. 6. In each case the three plots moving from top to bottom are respectively at $t = 0$, $t = 300$, and $t = 600$ orbits. The changing orientation of the disc, viewed from the original fixed coordinate system, as a function of time, as well as the location of the planet and gap is displayed. Note that the planet is not seen in the uppermost of the lower set of plots because it is located on the y axis. The unit of length is 5 AU and the surface density indicated in the colour bar is given in $M_J/(5\text{AU})^2$.

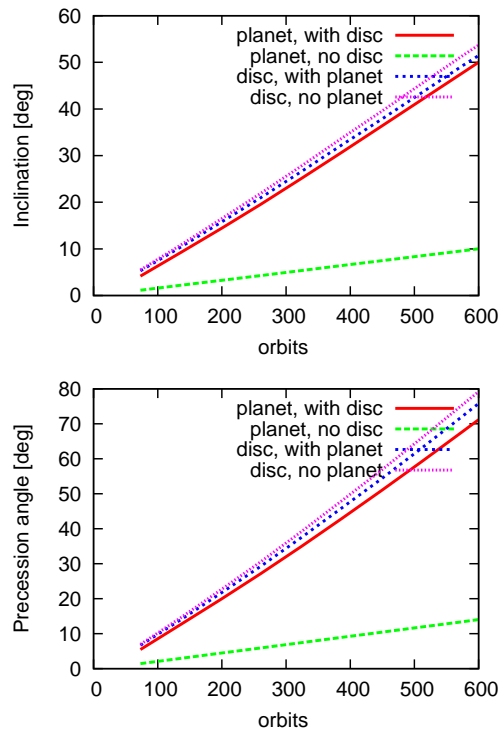


Figure 8. As in Fig. 6 but for a planet of mass $1 M_J$.

5.3 Simulations with a $1 M_J$ planet

The previous simulations incorporated a planet of mass $M_p = 2 M_J$. In this section, we give results for a planet of mass $1 M_J$, showing that the same conclusions regarding the coupling of planet and disc apply.

Fig. 8 shows the evolution of the inclination with respect to the (x, y) plane (upper panel) and precession angle (lower panel) of the planetary orbit and disc for a simulation for which both components were included and two simulations for which each component was considered alone. Again, the evolution of the disc orientation is not significantly affected by the planet. In contrast, the evolution of the planetary orbit orientation and its precession is accelerated by the disc. Compared to the $2 M_J$ case, the lower mass planet appears to be more tightly coupled to the disc when that is present. In general the system is found to behave similarly to the system with a $2 M_J$ planet.

5.4 Adiabatic removal of the binary star

When the binary companion is only present temporarily, as long as the removal process has a long characteristic time scale, as would be expected, for example, if it were associated with an accumulation of stochastic perturbations that might be produced in a star cluster we would expect the disc-planet system to respond adiabatically. The result could then be found by combining simulations for fixed binary orbits of the type carried out here.

Although we consider circular orbits, we remark that our results indicate that the dominant effect of the companion arises through the quadrupole term in the expansion of its time averaged perturbing potential at large dis-

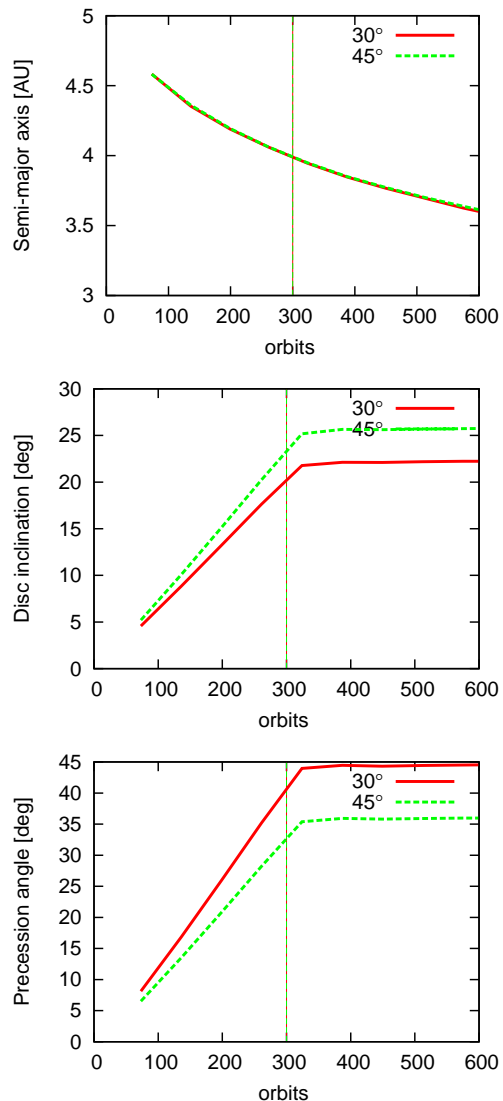


Figure 9. The evolution of the semi-major axis of the planet (top panel), the disc inclination to the (x, y) plane (middle panel), and the disc precession angle (bottom panel) when the mass of the binary companion star is gradually reduced to zero after 300 orbits. Results for $i_B = 30^\circ$ and 45° are shown.

tances. This term takes the same form for an eccentric orbit provided D is replaced by $A_B(1 - e_B^2)$, where A_B and e_B are its semi-major axis and eccentricity respectively (eg. Yokoyama et al. 2003). Accordingly we expect our results to have a wider application.

In order to study this, we ran test simulations in which the mass of the binary star was slowly reduced over a period of 50 orbits. for $i_B = 30^\circ$ and $i_B = 45^\circ$. Although this removal time exceeds the characteristic dynamical time in the disc, it is similar to but not long compared to the binary orbital period. Even so the disc-planet system adjusts adiabatically showing no evidence of impulsive kicks.

In Figure 9, the evolution of the semi-major axis of the planet, the inclination of the disc to the (x, y) plane and the disc precession angle is shown. The vertical lines mark the starting time of initiation of the reduction of the binary companion mass. For both $i_B = 30^\circ$ (red lines)

and $i_B = 45^\circ$ (green lines), this is after $t = 300$ orbits. The semi-major axis of the planet decreases smoothly as a result of inward migration. The binary companion mass reduction does not affect this plot since the relative orientation of the planet and disc stays constant throughout. In contrast to the semi-major axis, the disc inclination to the (x, y) plane and its precession angle are affected by the removal of the binary star. When the binary companion has been removed, it no longer exerts a torque on the disc. As a consequence, both the disc inclination to the (x, y) plane and its precession angle become constant. The adjustment occurs smoothly indicating an adiabatic process.

6 MULTIPLE PLANETARY SYSTEMS

We also study a planetary system composed of three planets, with masses 0.4, 1 and 2 M_J . The innermost planet with 0.4 M_J is put at 5 AU. The planets are initiated on circular orbits that are coplanar with the initial disc plane ($z = 0$). The outer two planets are put on circular orbits respectively of radii 7.122AU and 12AU. This makes the system close to a 2:3:6 resonance, being slightly outside it, so that convergent migration would be expected to move them towards it. In practice a 2:1 resonance eventually forms between the outermost pair of planets. However, the innermost pair does not attain an orbital resonance. After migration, the planetary system attains a state that is quite close to instability that can be induced when the system is perturbed. This is seen when the binary companion is introduced (see below).

6.1 Comparison of results obtained with SPH and a grid based code

As a first step, we compare the evolution of the three planets using the N-body/SPH code GADGET2 and a grid based code without the inclusion of a binary companion. We performed two dimensional simulations using the grid based code NIRVANA (see eg. Nelson et al. 2000, and references therein). Because they are of necessity 2D, these simulations can only be carried out for coplanar systems with no relative orbital inclinations. We adopted a 500×576 equally spaced grid in (r, ϕ) , finding that reducing the number of grid points in each direction by a factor of two did not result in significant changes over run times. An issue is that NIRVANA operates with fixed radial boundaries, which may be taken to be either rigid or open. These conditions do not mimic the behaviour of the SPH code which allows free outward expansion at large r , and a partial accumulation with some accretion near $r = 0$. We found that open boundary conditions resulted in too much material being lost and instead used partially open boundary conditions which reduced outflow speeds by a constant factor of 0.2 for the inner boundary, and 0.7 for the outer boundary, as compared to the fully open condition. We remark that the amount of material in the inner regions of the disc is sensitive to these conditions and this can affect the inward migration of giant planets (see eg. Crida et al. 2008). Given these complications, nonetheless we confirm that the very different numerical procedures lead to characteristically similar outcomes. For the NIRVANA simulations the inner and outer boundary radii were taken to be 0.4 and 5 internal units respectively

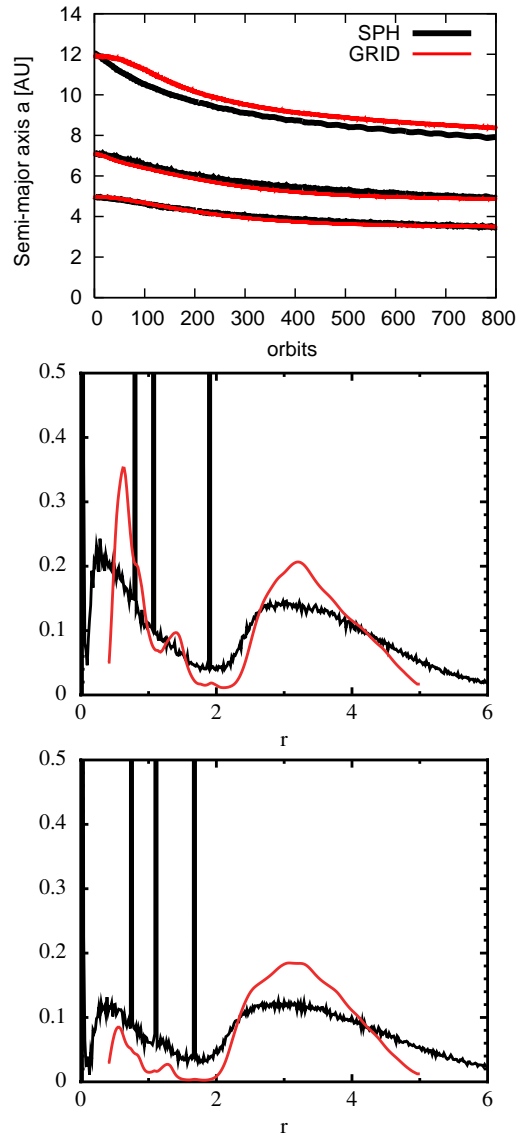


Figure 10. Comparison between SPH (black) and grid code (red lines). The upper panel shows the semi-major axes of the 3 planets embedded in a gas disc. The lower panels study the surface mass density profiles at two different times (see text). The prominent spikes are due to mass accumulation in the vicinity of the planets.

The softening parameter for the planet potentials was taken to be $0.6H$. The initial surface density profile, initial planet parameters and circumprimary disc aspect ratio were chosen to be the same as for the SPH code as indicated above. The kinematic viscosity was taken to be constant with a scaling such that $\alpha_{SS} = 0.006$ at a distance of one internal unit from the central star. This value is somewhat smaller than the value inferred from ring spreading tests. However, we found that a run for which the viscosity was increased by a factor of three led to very similar migration of the planets. In these simulations this depends on the distribution of the embedding material as well as an effective viscosity which is operating under different circumstances to those in a ring spreading test.

Tests have shown that the mass of the disc is the main parameter affecting the migration rate of the planets. In this

context we note that the masses of the two components (disc and planets) contained within a radial scale characteristic of the outermost planet’s orbital radius are initially comparable. The local disc mass subsequently decreases as mass flows towards the star. Since (at least) the outer two planets are on resonant orbits they migrate together with the disc which becomes increasingly unable to drive the migration of the planets due to its small mass compared to the total mass of all the planets. In addition material tends to accumulate in an inner disc interior to the planets which tends to counteract inward migration driven by the outermost planet.

In the case of the SPH code, the disc is allowed to evolve in the presence of the three planets for 100 orbits before planetary migration is switched on. By doing this, we allow the disc to smooth out its initial small-scale fluctuations and we allow the planets to open gaps in the disc. In the plot of the semi-major axis evolution in the uppermost panel of Fig. 10, the initial 100 orbits are not shown for the SPH simulation, i.e. the simulation starting time shown is the time after the initial 100 orbits when the planets start to migrate. In contrast, in the case of NIRVANA, the planetary migration is activated from the simulation start. The plot shows that the evolution of the semi-major axes of the planets is comparable for both codes. Only for the outer most massive planet, is there a small difference between the two simulations. The reason for this could be the depth of the gap. For a $2 M_J$ planet, NIRVANA shows a deep gap while the SPH code is not able to produce such a deep gap. The excess of material in its neighbourhood would be expected to lead to a slightly faster inward migration of the massive planet during the early stage of the simulation.

The plots in the middle and bottom panels of Fig. 10 compare the surface densities after 280 and 560 orbits respectively. The black lines show the SPH results while the red lines shows the results from NIRVANA. The surface density profiles reveal some differences. The fixed outer boundary for NIRVANA is at 5 internal length units (25 AU) beyond which there is no gas. In contrast, the SPH code allows the gas disc to expand freely with the outer disc edge becoming increasingly smeared out. In addition the gaps associated with the two most massive planets, of 1 and $2 M_J$ respectively, are deeper for NIRVANA than for the SPH case. This is a known characteristic difference between grid based and SPH codes and it has been noted by previous authors (e.g. de Val-Borro et al. 2006). The inner disc boundary is treated differently by the two codes. In the SPH case, particles enter the accretion region around the star, some of which are accreted and then removed from the simulation. The inner boundary of the grid based code is partially open with material passing through it being lost. This was taken to be at 0.4 internal units (2AU) for numerical convenience. The consequence is that there is more accumulation of material in the central regions in the SPH simulation which can eventually affect the inwardly migrating planets.

6.2 The effect of an inclined binary orbit

We now describe a SPH simulation starting with the same parameters as that described in the previous section but now including a $1M_\odot$ binary companion in circular orbit with $i_B = 45^\circ$. Results are presented in Fig. 11. In this simulation the planetary system is ultimately unstable. Instability

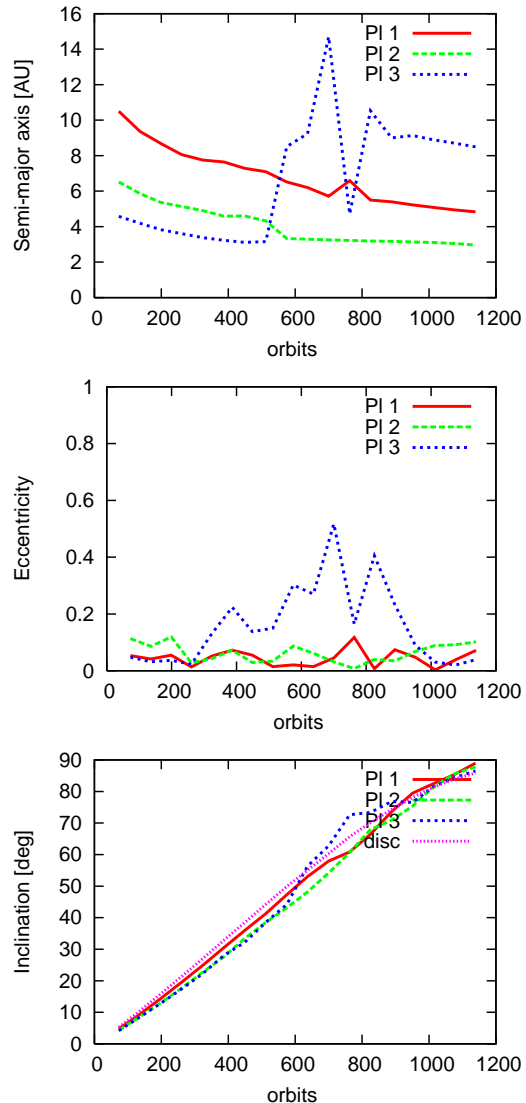


Figure 11. Evolution of a 3 planet system embedded in a gas disc and perturbed by a binary companion with $i_B = 45^\circ$ and $D = 100$ AU. The semi-major axes, eccentricities and inclinations with respect to the (x, y) plane of the three planets are shown in the top, middle and bottom panels respectively. The corresponding inclination of the disc is also shown in the bottom panel. The initially outermost, central and innermost planets are labelled by PI 1, PI 2 and PI 3 respectively.

starts after 500 orbits and leads to close encounters between the planets. The interactions produce a new radial ordering of the planets. The innermost planet with $M_p = 0.4 M_J$ is scattered outwards to become the outermost planet. After an additional scattering, the three planets stabilize in near circular orbits after ~ 900 orbits. Although the planetary system is unstable, its inclination with respect to the $z = 0$ plane and its relative inclination with respect to the binary companion, remain coupled to the disc as for the single planet cases throughout the evolution. The evolution of precession angles of the components of the planetary system are shown in Figure 12. This reveals the same characteristic evolution as previous simulations with just one planet. In the presence of the gas disc, the precession of the planetary

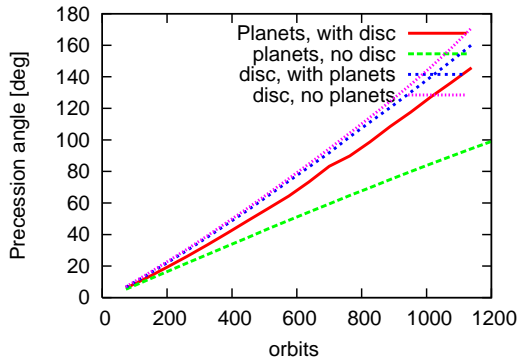


Figure 12. Precession angles for the components of the simulation shown in Fig. 11 together with precession angles obtained from simulations where the disc and planetary system were included individually without the other component. As in the latter case migration did not occur the planetary system did not undergo an instability.

angular momentum vector occurs significantly faster than it does in the absence of the gas disc. The observed precession of the disc with the planets is almost identical to that observed when the planets are absent.

7 SUMMARY AND DISCUSSION

We have performed SPH-simulations in order to study the influence of a stellar binary companion on a circumstellar disc and massive planets that may orbit therein. The gas disc and the planets were initiated on coplanar circular orbits around the central star. We studied four inclinations of the plane of the binary orbit to the initial disc midplane. These were $i_B = [30^\circ, 45^\circ, 60^\circ \text{ and } 80^\circ]$. The masses of the central star and binary companion were taken to be $1 M_\odot$. We considered planets of mass $2 M_J$ and $1 M_J$ in a disc of mass $0.01 M_\odot$ with outer radial boundary at 20 AU. The binary orbit was taken to be circular with orbital radius 100 AU.

The central finding was that the planet and the gas disc evolved maintaining approximate coplanarity for the full range of i_B . Apart from the geometric configuration of the orbits, this coplanarity was manifested in diverse ways, such as the invariance of the inward planet migration or the gap profile. Importantly and quite generally, the relative inclination of the disc and planet in respect to the binary star was constant through the simulations. The enforcement of coplanarity means that large inclination changes between the plane of the disc-planet system and the original disc plane, which might coincide with the stellar equatorial plane, can attain large values, especially for large i_B . Such changes could be made permanent if the binary companion is removed.

We remark that we have neglected any precessional or accretion torques acting on the central star which might change the orientation of its equatorial plane. However, Batygin (2012) showed that precessional torques could be neglected for a slowly rotating star when the disc extended down to the corotation radius. Furthermore, they are expected to be significantly weaker for a disc with an inner cavity as envisaged here. Accretion torques are also likely to be

weak in these circumstances and notably Batygin & Adams (2013) indicate that these depend on the form of the stellar magnetic field and do not need to act in a way that would tend to make the system align.

Although the specific choice of simulation parameters relating to the initial disc size and binary orbit were chosen largely for numerical convenience, we point out that the results can be extended to apply to other configurations in a number of ways. Apart from being able to apply the usual scaling of lengths and times that leave gravitationally interacting systems invariant, we remark that the important perturbation component from the binary companion that is responsible for precession and orbital orientation changes is the time averaged quadrupole term that is dominant for large orbital separation. This term takes the same form regardless of the eccentricity of the orbit, provided D is replaced by $A_B(1 - e_B^2)$, where A_B and e_B are the semi-major axis and eccentricity of the binary orbit respectively. Thus, as long as the quadrupole term is dominant we expect similar results. In addition, we estimated the precession period from our simulations to be $3.8 \times 10^4 (20\text{AU}/R_{out})^{3/2} (D/100\text{AU})^{3/2}$ yr (see Section 4.1). Thus the same precession period is obtained if R_{out} and D are increased by the same factor. Although the disc is larger, the dynamics in the inner region should not be affected as long as internal communication in the disc allows quasi-rigid body precession. Note too that if we increase D without increasing R_{out} , the precession period increases making the maintenance of coplanarity even easier.

In summary, the main factors affecting the maintenance of coplanarity are the ability of the disc to communicate within a precession period and the ability of the components to exert strong enough precessional torques. These can be estimated from equations (A5)-(A11) and will be seen to be determined by the disc and planet parameters within a radial scale defined by the planetary system rather than the outer boundary radius. This generates many possibilities for producing significant orbital reorientation through interaction with the binary.

Furthermore we also ran test simulations in order to model the slow removal of the binary companion. By doing this, we noted the adiabatic behaviour of the system. We found a smooth transition of the system to one with only a central star. Due to the lack of the external torque, the system stopped its precession, attaining a constant inclination between the midplane of the disc-planet system and the original disc midplane. This indicates that large orbital orientation changes could be produced through a sequence of interactions with different binary companions as long as the dynamical processes associated with evolution of the binary orbits is long compared to the characteristic dynamical time.

We also studied a multi-planet system with three planets and disc under the influence of a binary companion. We performed a comparison between the N-body/SPH code GADGET-2 and a 2D grid based code NIRVANA for the system with no binary companion. The planets with masses 0.4, 1 and $2 M_J$ were put on coplanar circular orbits near to a 2:3:6 resonance. Even though there are significant differences in implementation such as the treatment of the boundary conditions and the application and behaviour of viscosity,

the form of the migration of the planets is in satisfactory agreement.

When the planetary system was embedded in a gas disc in the presence of a binary companion, it was found that inward migration resulted in the appearance of instability. After 500 orbits, the innermost planet of $0.4 M_J$ was scattered to attain the outermost orbit after which the evolution stabilized with the planets again attaining near circular orbits. Throughout this evolution, the orbital inclinations of all three planets remained strongly coupled to the disc inclination. In this respect the multi-planet system behaved exactly as the single planet system.

Thus the simulations that we have performed have shown that when the disc is induced to undergo quasi-rigid body precession, as long as this is on a long enough timescale that internal precessional torques can retain coplanarity. This is maintained when there is a migrating planetary system with gaps in the interior part of the disc.

In this regard, we remark that Ghez et al. (1993) have conducted an observational survey of T Tauri stars in two neighbouring star forming regions and obtained a binary frequency in the separation range 16 - 252 AU for T Tauri stars of $\sim 60\%$ which is roughly 4 times greater than the binary star frequency for solar-type main-sequence stars. As this frequency can be altered by evolutionary processes within star clusters which can form and disrupt binary systems, Ghez et al. (1993) proposed that the high binary star frequency associated with T Tauri stars is correlated with their young ages and is thus an evolutionary effect. However, this could be crucial for a protoplanetary disc, since as shown in our simulations, an inclined binary companion is able to produce a disc with a high inclination with respect to the stellar equatorial plane in a time that is short compared to the disc's lifetime. More recent studies of binaries in young stellar systems mainly support the results of Ghez et al. (1993) (e.g. Köhler 2001; Kraus & Hillenbrand 2007; Kroupa 2011). Although there is a large uncertainty, observations reveal a frequency of binary systems in stellar clusters of $30 \sim 50\%$ (Duchene et al. 2004; Kraus & Hillenbrand 2009; Marks & Kroupa 2012). Note that this is comparable to the frequency of hot Jupiters with orbits that are highly inclined with respect to the stellar equatorial plane. Given the high abundance of binary stellar systems and the short timescale required for inclination generation, a scenario involving a binary companion with separation of the order of 100 AU could accordingly give a possible explanation for the observed frequency of planets on highly inclined orbits.

ACKNOWLEDGMENTS

Xiang-Gruess acknowledges support through Leopoldina fellowship programme (fellowship number LPDS 2009-50). Simulations were performed using the Darwin Supercomputer of the University of Cambridge High Performance Computing Service, provided by Dell Inc. using Strategic Research Infrastructure Funding from the Higher Education Funding Council for England and funding from the Science and Technology Facilities Council.

REFERENCES

- Albrecht S., Winn J. N., Johnson J. A., Howard A. W., Marcy G. W., Butler R. P., Arriagada P., Crane J. D., Shectman S. A., Thompson I. B., Hirano T., Bakos G., Hartman J. D., 2012, *ApJ*, 757, 18
- Bate M. R., Bonnell I. A., Price N. M., 1995, *MNRAS*, 277, 362
- Bate M. R., Lodato G., Pringle J.E., 2010, *MNRAS*, 401, 1505
- Batygin K., *Nature*, 491, 418
- Batygin K., Adams F.C., *ApJ*, 778, 169
- Bitsch B. & Kley W., 2011, *A&A*, 530, A41
- Cresswell P., Dirksen G., Kley W., Nelson R. P., 2007, *A&A*, 473, 329
- Crida, A., Sandor, Z., Kley, W., 2008, *A&A*, 483, 325
- Dawson R. I., Murray-Clay R. A., 2013, *ApJ*, 767, L24
- de Val-Borro M. et al., 2006, *MNRAS*, 370, 529
- Duchene G., Bouvier J., Bontemps S., Andre P., Motte F., 2004, *A&A*, 427, 651
- Fabrycky D. & Termain S., 2007, *ApJ*, 669, 1298
- Ghez, A. M.; Neugebauer, G.; Matthews, K., 1993, *AJ*, 106, 2005
- Huber D., Carter J. A., Barbieri M., Miglio A., Deck K. M. et al., 2013, *Science*, doi:10.1126/science.1242066, arXiv:1310.4503
- Köhler R., 2001, *AJ*, 122, 3325
- Kraus A. L. & Hillenbrand L. A., 2007, *ApJ*, 662, 413
- Kraus A. L. & Hillenbrand L. A., 2009, *ApJ*, 703, 1511
- Kroupa P., 2011, in *Computational Star Formation*, ed. J. Alves & B. J. Elmegreen, IAU Symp., 270, 141
- Larwood J. D., Nelson R. P., Papaloizou J. C. B., Terquem C., 1996, *MNRAS*, 282, 597
- Marks M. & Kroupa P., 2012, *A&A*, 543, A8
- Marzari F. & Nelson A. F., 2009, *ApJ*, 705, 1575
- Mayer L., Quinn T., Wadsley J., Stadel J., 2002, *Science*, 298, 1756
- Mizuno H., 1980, *Progress of Theoretical Physics*, 64, 544
- Nagasawa M., Ida S., Bessho T., 2008, *ApJ*, 678, 498
- Nelson, R. P., Papaloizou, J. C. B., Masset, F., Kley, W., 2000, *MNRAS*, 318, 18
- Papaloizou, J. C. B., Lin, D. N. C., 1999, *ApJ*, 438, 841
- Papaloizou J. C. B. & Terquem C., 1995, *MNRAS*, 274, 987
- Papaloizou J. C. B. & Terquem C., 2001, *MNRAS*, 325, 221
- Peplinski A., Artymowicz P., Mellema G., 2008, *MNRAS*, 386, 164
- Pollack J. B., Hubickyj, O., Bodenheimer P., Lissauer J. J., Podolak M., Greenzweig Y., 1996, *Icarus*, 124, 62
- Rasio F. A. & Ford E. B., 1996, *Science*, 274, 954
- Rein H., 2012, *MNRAS*, 422, 3611
- Schäfer C., Speith R., Hipp M., Kley W., 2004, *A&A*, 418, 325
- Shakura, N. I., Sunyaev, R. A., 1973, *A&A*, 24, 337
- Springel V., 2005, *MNRAS*, 364, 1105
- Terquem C., 2013, *MNRAS*,
- Teyssandier J., Terquem C., Papaloizou J. C. B., 2013, *MNRAS*, 428, 658
- Thies I., Kroupa P., Goodwin S. P., Stamatellos D., Whitworth A. P., 2011, *MNRAS*, 417, 1817
- Thommes, Lissauer, 2003, *ApJ*, 597, 566
- Triaud A. H. M. J. et al., 2010, *A&A*, 524, A25

- Weidenschilling S. J. & Marzari F., 1996, *Nature*, 384, 619
 Wu Y., Murray N. W., Ramsahai J. M., 2007, *ApJ*, 670, 820
 Xiang-Gruess M. & Papaloizou J. C. B., 2013, *MNRAS*, 431, 1320
 Yokoyama, T., Santos, M. T., Cardin, G., Winter, O. C., 2003, *A&A*, 401, 763

APPENDIX A: CONDITIONS FOR UNIFORM PRECESSION

We consider the conditions for a system consisting of a disc and an interior planetary system to precess uniformly together while maintaining only a small relative inclination under perturbation from an object such as an external binary companion. A complete treatment requires an analysis of the internal dynamics of disk warping together with the response of the planetary orbits (eg. Larwood et al. 1996, Terquem et al., 1998). However, such a discussion is complex and as we require only approximate estimates, we shall consider a simplified approach based on estimating whether the magnitudes of gravitational torques between different components of the system can be sufficient to enable it to precess as a whole while maintaining approximate coplanarity. We proceed by assuming the latter situation occurs and then consider whether it can be maintained by internal torques.

We adopt a simple model for which only secular interactions are considered. Thus possible effects arising from orbital resonances are neglected. We also ignore the effects of density waves excited through disc-planet interactions, making the assumption that the disc mass distribution is unperturbed. Nonetheless the torque balance we consider should still occur. The approach can be applied to situations where planets are within a disc gap or inner cavity or where there is no disc.

An illustration of the type of situation we study is given in Fig. A1. We consider two components of the disc-planet system undergoing precession induced by a binary companion. This is presumed to occur while it maintains an approximate planar structure. However, only the outer component is directly induced to precess by the binary companion. The inner component has to adjust a relatively small mutual inclination so that the torque acting on it due to the outer component causes it to precess at the same rate. As illustrated in Fig. A1 this requires that the components of the angular velocity of precession induced by the mutual interaction, and the angular velocity of precession of the entire system, that are perpendicular to the angular momentum vector of the inner component be the same. This is because it is only these components that determine the rotation rate of the latter vector.

We remark that many studies (eg. Larwood et al. 1996) have shown that a gaseous disc can maintain uniform precession under the action of torques due to a binary companion, provided that sonic or diffusive communication can occur within a precession time scale. These conditions are satisfied for our simulations and disc self-gravity is not required. Here we focus on the incorporation of an inner planetary system, which on account of depletion of material through

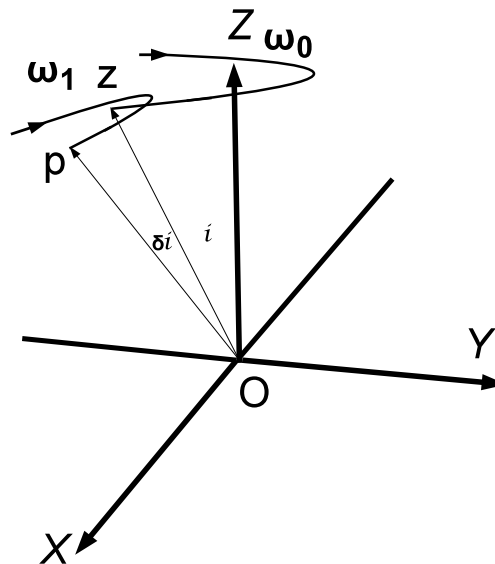


Figure A1. Schematic illustration of the precession of the different components of a disc-planet system. A binary companion causes the total angular momentum of the inclined system to precess around the binary orbital angular momentum vector in the direction OZ , with precession angular velocity ω_0 . The torque from the binary is too weak to affect the inner planetary system whose angular momentum vector in the direction Op , is induced to precess about the total angular momentum vector of the disc-planet system in the direction Oz , with precession angular velocity ω_1 , through the action of disc-planet, or planet-planet torques. The angular momentum vectors are maintained in the same plane if the components of the precession angular velocity vectors, ω_0 and ω_1 perpendicular to Op are the same. This requires the inclinations to be adjusted so that $|\omega_0| \sin(i + \delta i) = |\omega_1| \sin \delta i$. This results in a small mutual inclination, δi , provided $|\omega_1| \gg |\omega_0|$.

gap formation is expected to require gravitational torques in order to maintain coupling to the outer disc.

As the precession frequencies of interest are much smaller than the characteristic orbital frequency, we average over many orbits so that the system, incorporating any planets present, may be considered to consist of a mass distribution. Assuming orbits to be circular, both for planets and in the disc, this may be taken to be a combination of distributions, each of which may be taken to be axisymmetric with appropriate symmetry axes. We now discuss the torques between such distributions and the induced precession rates.

A1 Precessional torques induced by axisymmetric mass distributions

We consider the precessional torque acting between two mutually inclined axisymmetric mass distributions. The densities associated with these are respectively taken to be $\rho_1(\mathbf{r})$ and $\rho_2(\mathbf{r})$. We adopt cylindrical coordinates (R, ϕ, z) such

that the symmetry axis associated with $\rho_1(\mathbf{r})$ is the z axis. The (x, y) plane is assumed to be a plane of symmetry such that $\rho_1(R, -z) = \rho_1(R, z)$. The distribution associated with $\rho_2(\mathbf{r})$ has the same symmetry properties but the plane of symmetry is taken to have an inclination δi with respect to the (x, y) plane and accordingly the axis of symmetry is inclined at an angle δi to the z axis. We shall assume the distribution $\rho_1(\mathbf{r})$ is located exterior to the distribution $\rho_2(\mathbf{r})$. In addition the x axis is chosen such that the two symmetry planes intersect on it.

There will be a torque of magnitude, T_{12x} , between these distributions acting in the x direction. This acts to produce precession about their total angular momentum axis. We shall assume that the outer distribution associated with $\rho_1(\mathbf{r})$ contains almost all the angular momentum so that the precession will be about the z axis. The torque magnitude T_{12x} is readily written down as

$$T_{12x} = - \int \rho_2(\mathbf{r}) \left(y \frac{\partial \Psi_1}{\partial z} - z \frac{\partial \Psi_1}{\partial y} \right) d^3 \mathbf{r}, \quad (\text{A1})$$

where Ψ_1 is the gravitational potential arising from $\rho_1(\mathbf{r})$ and this and similar integrals below are taken over the domains occupied by the relevant mass distribution. Substituting for Ψ_1 , we find

$$T_{12x} = - \iint G \rho_2(\mathbf{r}) \rho_1(\mathbf{r}') \frac{(zy' - yz')}{|\mathbf{r} - \mathbf{r}'|^3} d^3 \mathbf{r}' d^3 \mathbf{r}. \quad (\text{A2})$$

We assume that $\rho_1(\mathbf{r})$ is confined to the plane $z = 0$ forming a distribution appropriate to a flat disc, while $\rho_2(\mathbf{r})$ is confined to a ring corresponding to the time averaged mass distribution appropriate to a planet on a circular orbit. Then (A2) reduces to

$$T_{12x} = - \frac{GM_{p,2} r_{p,2} \sin \delta i}{2\pi} \times \iiint \frac{R^2 \Sigma(R) \sin \psi \sin \phi d\psi d\phi dR}{(R^2 + r_{p,2}^2 - 2Rr_{p,2} \cos \alpha)^{3/2}}, \quad (\text{A3})$$

where $\cos \alpha = \cos \phi \cos \psi + \sin \phi \sin \psi \cos \delta i$, Σ is the disc surface density, the mass of the planet is $M_{p,2}$ and its orbital radius is $r_{p,2}$. When Σ is assumed to be localized at radius, $r_{p,1}$, such that the total associated mass is $M_{p,1}$, the torque becomes that acting between two planets of masses $M_{p,1}$ and $M_{p,2}$, namely

$$T_{12px} = - \frac{GM_{p,1} M_{p,2} r_{p,1} r_{p,2} \sin \delta i}{4\pi^2} \times \iint \frac{\sin \psi \sin \phi d\psi d\phi}{(r_{p,1}^2 + r_{p,2}^2 - 2r_{p,1} r_{p,2} \cos \alpha)^{3/2}}. \quad (\text{A4})$$

In the limit of small δi , which is of interest as it corresponds to close alignment, $\cos \delta i$ may be replaced by unity in the expression for $\cos \alpha$ and the integrals over the angles may be carried out with the result that

$$T_{12x} = - \frac{1}{2} \pi G M_{p,2} r_{p,2} \sin \delta i \int \frac{\Sigma(R) b_{3/2}^1(r_{p,2}/R)}{R} dR, \quad (\text{A5})$$

with the Laplace coefficient is defined through

$$b_{3/2}^1(x) = \frac{1}{\pi} \int \frac{\cos \alpha d\alpha}{(1 + x^2 - 2x \cos \alpha)^{3/2}}. \quad (\text{A6})$$

The corresponding expression for two planets of masses $M_{p,1}$

and $M_{p,2}$ is

$$T_{12px} = - \frac{GM_{p,1} M_{p,2} r_{p,2} \sin \delta i}{4r_{p,1}^2} b_{3/2}^1(r_{p,2}/r_{p,1}). \quad (\text{A7})$$

Lower bounds for the absolute magnitudes of the torques can be estimated by replacing $b_{3/2}^1(x)$ by the first term in its series expansion, namely $3x$. Thus for a model disc with $\Sigma \propto R^{-1/2}$ truncated at an inner radius, $R_{in,d}$, assumed to be much less than its outer truncation radius, R_{out} , we integrate (A5) over R to estimate the torque exerted by the disc on the planet with mass $M_{p,2}$ to be

$$T_{12x} \sim - \frac{3GM_D M_{p,2} r_{p,2}^2 \sin \delta i}{4(R_{out} R_{in,d})^{3/2}}. \quad (\text{A8})$$

A2 Precession frequencies

The retrograde precession rate induced in the orbit $M_{p,2}$ by the disc is readily found from

$$\omega_{p2} = \frac{|T_{12x}|}{M_{p,2} r_{p,2}^2 \Omega_{p,2} \sin \delta i}, \quad (\text{A9})$$

where $\Omega_{p,2}$ is the orbital frequency of $M_{p,2}$. Using equation (A8), we obtain the estimate

$$\frac{\omega_{p2}}{\Omega_0} \sim \frac{3M_D}{4M_\odot} \frac{r_{p,2}^{3/2} R_0^{3/2}}{(R_{out} R_{in,d})^{3/2}}, \quad (\text{A10})$$

In the case of a planetary system, uniform precession of the innermost planets may be maintained through torques due to other planets. We now suppose $M_{p,2}$ is acted on by an exterior planet $M_{p,1}$. Replacing T_{12x} in equation (A9) by T_{12px} given by equation (A7) we estimate the retrograde precession frequency induced by $M_{p,1}$ on $M_{p,2}$ to be

$$\frac{\omega_{p2}}{\Omega_0} = \frac{M_{p,1} r_{p,2}^{1/2} R_0^{3/2}}{4M_\odot r_{p,1}^2} b_{3/2}^1(r_{p,2}/r_{p,1}). \quad (\text{A11})$$